Anal Bioanal Chem (2011) 399:1455–1465
DOI 10.1007/s00216-010-4438-5

ORIGINAL PAPER

Size separations of starch of different botanical origin studied by asymmetrical-flow field-flow fractionation and multiangle light scattering

Karl-Gustav Wahlund · Mats Leeman · Stalin Santacruz

Received: 3 July 2010 / Revised: 9 November 2010 / Accepted: 12 November 2010 / Published online: 22 December 2010

Abstract Asymmetrical-flow field-flow fractionation combined with multiangle light scattering and refractive index detection has been revealed to be a powerful tool for starch characterization. It is based on size separation according to the hydrodynamic diameter of the starch components. Starch from a wide range of different botanical sources were studied, including normal starch and high-amylose and high-amylopectin starch. The starch was dissolved by heat treatment at elevated pressure in a laboratory autoclave. This gave clear solutions with no granular residues. Amylose retrogradation was prevented by using freshly dissolved samples. Programmed cross flow starting at 1.0 mL min^{-1} and decreasing exponentially with a half-life of 4 min was utilised. The starches showed two size populations representing mainly amylose and mainly amylopectin with an overlapping region where amylose and amylopectin were possibly co-eluted. Most of the first population had molar masses below 10^6 g mol^{-1}, and most of the second size population had molar masses above 10^7 g mol^{-1}. Large differences were found in the relative amounts of the two populations, the molar mass, and hydrodynamic diameters, depending on the plant source and its varieties.

Keywords Molar mass · Starch · Size separation · Hydrodynamic diameter · Field-flow fractionation · Multiangle light scattering

Published in the special issue *Separation Science of Macromolecules* with Guest Editor André Striegel.

K.-G. Wahlund (✉)
Technical Analytical Chemistry, Department of Chemistry,
Center for Chemistry and Chemical Engineering,
Faculty of Engineering LTH, Lund University,
P.O. Box 124, 221 00, Lund, Sweden
e-mail: karl-gustav.wahlund@analykem.lu.se

Present Address:
M. Leeman
MIP Technologies AB, A subsidiary of Biotage AB,
Box 737, 220 07, Lund, Sweden

Present Address:
S. Santacruz
Colegio de Agricultura Alimentos y Nutricion,
Universidad San Francisco de Quito,
Diego de Robles y Circulo Cumbaya,
P.O. Box 17-12-841, Quito, Ecuador

Introduction

Starch has two main components, amylose and amylopectin [1]. Amylose is mainly linear, composed of α-glucosyl units through 1→4 linkages. Amylopectin has a highly branched structure, in which the branching points are formed by an α (1→6) linkage. Amylose has a weight-average molar mass (M_w) that varies from 10^5 to 10^6 g mol^{-1}, whereas for amylopectin it varies from 10^7 to 10^9 g mol^{-1}. The molar mass distribution of starches has conventionally been determined by size-exclusion chromatography (SEC). However, materials with ultrahigh molar mass, for example amylopectin, will be eluted unresolved in the "excluded" volume and may also suffer from degradation due to shearing forces in the packed column bed. A successful unique analytical method, asymmetrical-flow field-flow fractionation (AsFlFFF), circumvents these drawbacks, because it is especially suited to rapid analytical size-separation of ultra-high-molar-mass biopolymers and bio-colloidal particles [2–7].

The separation in AsFlFFF is obtained along a thin open flow channel. A laminar flow of a liquid carrier with a parabolic flow profile results in elution of the sample

components at different retention times (elution times). The retention is the result of a transversal field, the crossflow, which concentrates the sample components close to one of the walls of the channel. This wall is made up of an ultrafiltration membrane across which the crossflow permeates. The method is generally suited to size separations of macromolecules and colloidal particles from 2 to 500 nm diameter. The size separation occurs because the retention time is inversely proportional to the diffusion coefficient of a sample component and the diffusion coefficient is dependent on the macromolecular or particle size and shape. Conversely, the diffusion coefficient of a sample component can be calculated from the observed experimental retention time and then transformed into the hydrodynamic diameter, which is an important characteristic of macromolecules.

When AsFlFFF is coupled on-line to a multiangle light-scattering (MALS) detector and a differential refractive index (RI) detector the molar mass and the root-mean-square radius can be directly measured. This substantially increases the amount of analytical information available. Thus determination of weight-average molar mass and distributions of rather small macromolecules (~10^4 g mol^{-1}) up to extremely large ones (>10^9 g mol^{-1}) becomes possible, and data on macromolecular conformation and shape are also obtained.

There are a few reports on the size separation of starch by use of different types of FFF. Lou et al. [8] achieved partial separation of amylose and amylopectin using thermal FFF. Sedimentation FFF has been used to characterize amylopectin starch [9, 10]. Roger et al. [11] successfully separated amylose and amylopectin in four maize starches of different amylose content (0, 30, 50, and 70%) using symmetrical-flow FFF with MALS–RI detection and a step programmed crossflow. In addition, a frit outlet with a split ratio of 1:1 was used to achieve enhanced detector signals. Dual flow programming of symmetrical-flow FFF for separation of amylose and amylopectin in maize has also been successful [12]. Another report [13] using symmetrical-flow FFF with programmed cross flow enabled successful separation of amylose from amylopectin in barley starch. Using asymmetrical-flow FFF Bruijnsvoort et al. [14] reported fractionation of amylopectin starch with MALS–RI detection. The amylopectin starch was partly eluted under lift/hyperlayer conditions and the reported sizes were therefore larger than those reported by Roger et al. [11]. A reasonable explanation of the larger size and very much higher molar masses could be that the dissolution procedure used did not completely dissolve all the starch. More recently, characterization of amylopectin starches from eight different botanical sources using asymmetrical-flow FFF has been reported [15].

Hence, rather little is known about the wider use of asymmetrical-flow field-flow fractionation in the characterization of natural starch, because the above mentioned publications focused on a rather narrow selection of starches. In this study 14 different starches from six botanical sources were screened. The objective was to separate the main components of starch, i.e. amylose and amylopectin, in a short time, and characterize the components in terms of their hydrodynamic diameter, weight-average molar mass, and z-average root-mean-square radius. Normal starch, high-amylose starch, and high-amylopectin starch were all evaluated. Potential applications are in evaluation of the character of starch macromolecules from different plant species and cultivars as support for understanding their technological properties.

Theory

Asymmetrical-flow field-flow fractionation (AsFlFFF)

A fundamental understanding and more complete description of asymmetrical-flow field-flow fractionation and its experimental implementation can be found in the literature [2–4, 16, 17]. For constant crossflow experiments it is possible to calculate the diffusion coefficient, D, of an eluted component from its elution time, t_r, if the cross-flow rate, F_c, and the channel dimensions are known, by use of:

$$D = \left(t^0 F_c w^2 / 6V^0\right) \cdot 1/t_r \tag{1}$$

where w is the channel thickness, V^0 the channel volume, and t^0 the void time (the time for an unretained component to be eluted from the channel). The void time can be calculated by use of [3]:

$$t^0 = \frac{V^0}{F_c} \ln\left(1 + \frac{F_c}{F_{out}}\left[1 - \frac{w\left(b_0 z' - \frac{b_0 - b_L}{2L} z' 2 - y\right)}{V^0}\right]\right) \tag{2}$$

where F_{out} is the flowrate through the outlet end of the channel and w the thickness of the trapezoidal channel. The terms b_0, b_L, L, z', and y are the breadth of the trapezoid at the inlet end, the breadth of the trapezoid at the outlet end, the length of the channel, and the distance from the channel inlet end to the point where the sample zone is focused immediately before the elution starts [3]. By combining Eq. (1) with the Stokes–Einstein equation a direct relationship between the hydrodynamic diameter, d_H, of a component and its retention (elution) time is obtained according to:

$$d_H = \left(2kTV^0 / \pi\eta t^0 F_c w^2\right) \cdot t_r \tag{3}$$

This shows that the hydrodynamic diameter of an eluted molecule can be experimentally determined directly from the observed retention time but also that sample compo-

nents will be eluted in order of increasing hydrodynamic diameter.

Although Eqs. (1)–(3) are valid for isocratic experiments only, where the crossflow rate is kept constant, the diffusion coefficient and the hydrodynamic diameter can still be calculated from the elution times in programmed runs after mathematical transformation. A full numerical solution for this purpose has been obtained [18] but in the present work a mathematically simpler method was applied. It is based on a modification of a previously described procedure that was used to predict the elution time for a component of given hydrodynamic diameter in programmed crossflow experiments [17]. The modified procedure is described in Supporting Information. As regards Eq. (2), which is valid for isocratic elution, it is still useable in this form for this study because the crossflow rate is constant during the first minute (Table 3 and Fig. 1).

Multiangle light scattering (MALS)

The amount of light scattered from a solution containing macromolecules depends on, among other things, the concentration of the macromolecules, the angle between the incoming light and the detector (the scattering angle), and the macromolecule molar mass and molecular size [19, 20]. The fundamental equation relating these parameters can be written as:

$$\frac{R_\theta}{Kc} = M_w P(\theta) \tag{4}$$

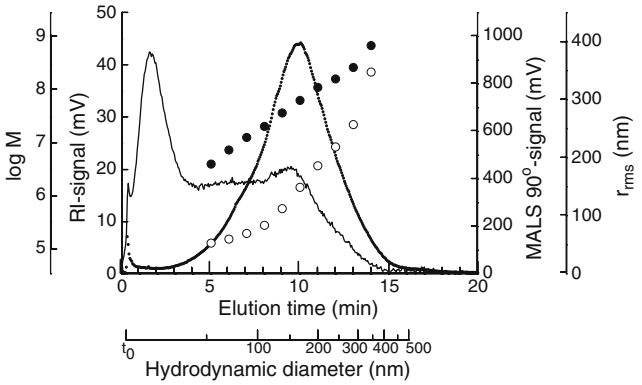

Fig. 1 Normal maize starch (Maize-1). RI-signal fractograms and MALS 90º fractograms of a maize starch of normal amylose content (maize-1). RI fractogram (*continuous line*), MALS 90º fractogram (*dotted line*), log M (= log $M_{w,slice}$) (*filled circles*), and r_{rms} (= $r_{rms,z,\ slice}$) (*open circles*). t_0= 0.3 min. The hydrodynamic diameters were calculated from the elution times ("Theory" section). For the very first eluted fractions no molar mass data were accessible because of the low MALS signal-to-noise ratio. $M_{w,slice}$ and $r_{rms,z,slice}$ were determined by use of Debye plots constructed at discrete elution times at even time intervals (1 min) across the fractograms where the MALS and RI signal-to-noise ratios were sufficient. The same procedure was used for all other starches

where R_θ is the Rayleigh ratio, which is proportional to the amount of scattered light at scattering angle θ, K an optical constant (affected by, among other things, the wavelength of the incoming light and the refractive index of the solvent), c the concentration (in weight) of the scattering molecule, M_w the weight-average molar mass, and $P(\theta)$ a particle scattering function. $P(\theta)$ depends in a complex way on the wavelength of the light, the scattering angle, and the z-average root-mean-square radius (z-average rms radius, $r_{rms,z}$). A so-called Debye plot is used to obtain M_w and $r_{rms,z}$. This procedure has been well described many times in the literature [21, 22].

The AsFlFFF channel can be coupled on-line to a MALS detector and an RI detector, both of which sample the eluate with high frequency. Then it is possible to determine $M_{w,\ slice}$ and $r_{rms,z,\ slice}$ in each narrow time fraction of the eluate, here termed a "slice". Thus it is possible to measure M_w and $r_{rms,z}$ of the complete macromolecule population, and also the molar mass and rms radius distributions.

Materials and methods

Starch samples

A large number of starches of different botanical origin were provided by various institutions and organisations participating in the project "Øresund Starch Profile" (ØSP) (Ministeriet for Videnskab, Teknologi og Udvikling, Sagsnr. 38968, Dok-id 144497, Denmark) which is a co-operation between Denmark and Sweden. Table 1 presents data on the starch samples studied. Their water content was determined by gravimetric analysis and subtracted in calculations of the analysed mass of starch, the value of which was used to calculate the recovery (Table 2).

Starch dissolution

Starch was dissolved by heat treatment at elevated pressure in a Roth Hochdruchlaborautoklav Modell II (Carl Roth, Karlsruhe, Germany) laboratory autoclave with a programmable temperature control unit. Starch (0.060 g) was dispersed in 60 g filtered (0.2 μm pore-size regenerated cellulose filter, order number 18407; Sartorius, Goettingen, Germany) de-ionised (Millipore, Bedford, MA, USA) water, directly in the autoclave vessel, furnishing a concentration of 0.1% (*w*/*w*). The starch dispersion was then flushed with nitrogen gas for 5 min (pressure approx. 10 bar) to avoid oxidative degradation of the sample when heated. The dispersion was then heated to 150°C from room temperature (approx.

Table 1 List of starch samples

Plant source and starch type	Provider	Label	Amylose content (%)[a]
Maize, normal, C Gel 03401	Cerestar-AKV I/S (Vodskov, Denmark)	Maize-1, OSP-1	29
Maize, high-amylose, C Gel 03003	Cerestar-AKV I/S (Vodskov, Denmark)	Maize-2, OSP-2	43
Maize, waxy, C Gel 04201, (high-amylopectin)	Cerestar-AKV I/S (Vodskov, Denmark)	Maize-3, OSP-3	0
Wheat, deglutinised R	Semper AB (Sundbyberg, Sweden)	Wheat-4, OSP-4	46
Wheat, deglutinised K	Semper AB (Sundbyberg, Sweden)	Wheat-5, OSP-5	45
Wheat, deglutinised E	Semper AB (Sundbyberg, Sweden)	Wheat-6, OSP-6	46
Rice, normal DR	KMC (Brande, Denmark)	Rice-10, OSP-10	16
Rice, high-amylopectin content, XS	KMC	Rice-11, OSP-11	0
Rice, normal B7	KMC	Rice-12, OSP-12	27
Potato, cultivar Kuras	AKV (Vodskov, Denmark)	Potato-7, OSP-7	28
Potato, transgenic low phosphate content variety of cultivar Dianella	Plant Biochemistry Laboratory, Royal Veterinary and Agricultural University (Frederiksberg, Denmark)	Potato-39, OSP-39	39
Potato, transgenic high-amylose content of cultivar Dianella	Plant Biochemistry Laboratory, Royal Veterinary and Agricultural University (Frederiksberg, Denmark)	Potato-40, OSP-40	41
Tapioca	KMC	Tapioca-8, OSP-8	31
Pea	KMC	Pea-9, OSP-9	57

[a]By the iodine-staining spectrophotometric method; data provided by the Department of AgroEcology, Crop Physiology and Soil Science, Danish Institute of Agricultural Sciences (Tjele, Denmark) within the Öresund Starch Profile

25°C) in approximately 15 min, then kept at 150 °C for 40 min (pressure approx. 17 bar), and after that cooled in a water bath to approximately 90°C and immediately analysed, i.e. within approximately 1–2 min. If not immediately analysed, such as for a series of triplicates, the samples were stored for no more than two hours in an oven at 90 °C until analysis. Samples were analysed on the same day they were prepared. All samples were analysed in duplicate, at least

Starch sample purity and integrity

The starch samples may contain traces of other components, for example protein, lipids, salts, high molar mass contaminants, water, etc. Proteins that are larger than the membrane cut-off (10 kDa) may co-elute with the starch components and affect determination of the molar mass. However because the protein content was below 1% its effect should be negligible. A frit with 2.0 μm pore-size

Table 2 Experimental recovery, hydrodynamic diameter (d_H), starch weight-average molar mass (M_w), and z-average rms radius ($r_{rms,z}$) for Population 2 determined by AsFlFFF–MALS–RI

Starch sample	Recovery (population 1+2) (%)[a]	Population 2		
		d_H (nm)	$M_w \times 10^{-8}$ (g mol^{-1})	$r_{rms,z} \times 10^{-2}$ (nm)
Maize-1	104	38–350	2.1	1.9
Maize-2	94	38–200	0.45	1.4
Maize-3	130	44–410	3.9	2.4
Wheat-4	107	53–350	2.1	2.3
Wheat-5	103	32–350	1.4	2.1
Wheat-6	101	32–350	2.4	2.3
Rice-10	108	45–450	4.5	3.2
Rice-11	105	24–550	3.9	2.3
Rice-12	86	32–450	3.5	2.5
Potato-7	117	41–410	1.1	2.0
Potato-39	127	53–350	0.9	1.8
Potato-40	112	45–350	2.0	2.4
Tapioca-8	118	32–330	0.61	1.5
Pea-9	115	50–500	1.8	2.5

[a]The large variability may primarily be because of difficulties in defining the baseline in the fractograms, because it did not reach zero

was placed in-line before the MALS detector to remove micron-sized particles that can clog the RI detector and increase the MALS signal-to-noise ratio (*S*/*N*). This precaution is essential because micro-particulate contaminants, even when present in small amounts, can seriously affect the MALS measurements. Low molar mass contaminants, smaller than the membrane cut-off, will most likely leave the separation channel through the ultrafiltration accumulation wall membrane and will therefore not interfere.

The dissolution temperature and time were chosen to obtain a degree of high dissolution, judged by the recovery (Table 2). An autoclaving temperature of 130°C was tested and optical microscopy showed the presence of granule residues, i.e. dissolution was not complete. After use of 150° C no presence of starch residues was observed by optical microscopy. To assess the risk of degradation a longer autoclaving time, 60 min, was tested. Signs of degradation (shift to lower elution time and reduced peak heights) were then observed, for which reason 40 min was chosen to reduce the risk of degradation. From other dissolution procedures it is known that degradation can occur [23]. A dissolution procedure in which complete dissolution would be ensured and polymer degradation avoided requires substantial efforts to optimize autoclave temperature and heating time. The choice of 150°C for 60 min for all starches in this study represents a compromise that aims at high dissolution degree and reduced risk of degradation. It is known [23] that starches of different botanical origin may need different dissolution conditions in DMSO. Therefore it is possible that precise optimum dissolution conditions in this study may be somewhat different for starches of different botanical origin and amylose/amylopectin ratio. It is, however, outside the scope of this work to optimize the dissolution for every starch.

Amylose is not stable in water because of retrogradation to its crystalline form producing aggregates that can precipitate. This must be prevented, and several approaches are used to minimize the problem. Dissolution of amylose in other solvents, for example DMSO, or dissolution in water and maintenance of high temperatures (>80 °C) have been reported [23, 24]. In this study retrogradation in water was hindered by keeping the samples in an oven at 90 °C until AsFlFFF-MALS-RI analysis. This procedure was assessed by recording MALS or RI fractograms from samples that were injected immediately after the dissolution and after storage at 90 °C for 45 min. No significant difference could be seen, which shows that the storage in the oven did not cause retrogradation of amylose nor did it cause any degradation of the starch. When samples were taken from the oven and restored to room temperature they were kept for no more than 1–2 min until injection into the AsFlFFF. This minimized the time during which amylose is present under conditions when retrogradation can occur, as has been reported by others [11, 13, 14]. Once inside the channel the starch becomes diluted to approximately 10^{-4} g mL^{-1} (i.e. ~0.01%) which is likely to help to further significantly reduce the risk of retrogradation. These precautions suggest there could not have been any significant retrogradation during the time period in which the analysis was performed. Therefore it is highly unlikely that retrogradation of amylose can have affected the results.

Instrumental

The asymmetrical-flow field-flow fractionation (AsFlFFF) instrument was an Eclipse F Separation System (Wyatt Technology, Santa Barbara, CA, USA). It was connected to a Dawn-DSP (Wyatt Technology) multiangle light-scattering photometer (MALS), with a laser wavelength of 632.8 nm, and an Optilab DSP interferometric refractometer (RI) detector (Wyatt Technology), using a wavelength of 632.8 nm. An Agilent 1100 series isocratic pump (Agilent Technologies, Waldbronn, Germany) with an in-line vacuum degasser was used to deliver the carrier to the system and an Agilent 1100 Series Autosampler to handle sample loading. A Teflon filter-holder with a 20 nm pore-size aluminium oxide filter (Anodisc 25; Whatman International, Maidstone, UK) was placed between the pump and the channel to ensure that particle-free carrier entered into the channel. A PEEK pre-column filter with a 2-μm PEEK frit (Upchurch Scientific, Oak Harbor, WA, USA) was placed between the channel and the MALS detector to remove large-sized particulate impurities.

The AsFlFFF channel was of the trapezoidal shape [3] and had a nominal thickness of 250 μm but was estimated to be 195 μm thick by measurement of the retention time of ferritin and pullulan standards having known diffusion coefficients [4]. The ultrafiltration membrane forming the accumulation wall was made of regenerated cellulose with a cut-off of 10 kDa (C010F; Nadir Filtration, Wuppertal, Germany).

The starch sample mass load was varied from 5 to 40 μg to check for any signs of overloading. Minor shifts in peak positions were observed but the resolution between separated fractions was not impaired. Therefore 40 μg was chosen (see below), because it was important to have a signal-to-noise ratio as high as possible.

All separations were made under the same experimental conditions using an exponentially decreasing programmed crossflow. The separation started at a flow rate of 0.40 mL min^{-1} for 1 min to rinse the sample loop. Sample solution, 40 μL, containing 40 μg starch was then injected followed by a 3-min focusing/relaxation step with a focusing flow rate of 1.0 mL min^{-1}. The crossflow started at 1.0 mL min^{-1} and then decreased step-wise approxi-

mately exponentially with a half-life of 4 min as shown in Table 3. The channel outlet flow rate through the detector was 1.0 mL min^{-1} and the void time 0.3 min.

A high-molar-mass pullulan standard was used as a control sample to check that the obtained molar mass and rms radius was correct.

Data evaluation

The MALS signal-to-noise ratio was quite low for the first eluted size population (mainly amylose) and much higher for the second eluted population (mainly amylopectin) for the reason that the light scattering signal sensitivity increases with increasing molar mass. This limited the elution time range over which the determination of M_w and $r_{rms,z}$ had acceptable precision. Hence, only the second population could be evaluated, as is illustrated in Fig. 1. Most often, the scattering data from the six lowest scattering angles (θ) above 26º were used. By using, in the Astra software (Wyatt Technology), the so called Debye plot, a linear function according to Berry's plotting method was fitted to the data. The software calculates the intercept and slope of the function by extrapolating to $\sin^2(\theta/2)=0$, which then enables the output of the weight-average molar mass ($M_{w,\ slice}$) and the z-average root-mean-square radius ($r_{rms,z,\ slice}$) at very short time increments across the total elution curve. From these data the weight-averaged molar mass, the *z*-averaged rms radius, and their distributions across the complete fractogram, or a certain time fraction thereof, were obtained. However, use of the Astra software to furnish molar masses and rms radii for the complete fractogram, i.e. the whole sample, requires that the same set of detector angles be used throughout the data processing. In several cases, however, optimum choices of detector angles had to be different in different elution time ranges of the fractogram, probably for the reason that the character (size and shape) of the polymers found in different size ranges may be very different. Then, a less automatic method was used in which the Debye plots were estimated at discrete points in 1-min time increments across the part of fractograms where the MALS and RI signal-to-noise ratios were sufficient. The resulting $M_{w,\ slice}$ and $r_{rms,z,\ slice}$ from each point were then plotted as illustrated in Fig. 1. To obtain the weight-average molar mass and the rms radius, 1st , 2nd, or 3rd-order polynomial fitting to the data points was performed by use of Excel spreadsheet software so that functions of molar mass vs. time and rms radius vs. time could be subjected to suitable integration.

A refractive index increment, d*n*/d*c*, for starch of 0.146 gmL^{-1} was taken from the literature [11, 13], and was used for all starch samples. The recovery of starch from the AsFlFFF was calculated by integration of the RI signal ("known d*n*/d*c* method" in the Astra software) and combination with the loaded mass of starch (after subtracting the water content). The d*n*/d*c* is assumed to be uniform over the size range of the fractionated polymer and independent of branching and botanical origin.

The second virial coefficient, the A_2 term, was unknown and set to zero, i.e. assuming it to be negligible. Because the concentration of the sample in the MALS cell was very low (<10^{-5} g mL^{-1}) this is a valid assumption. However, for amylopectin the molar mass is very high and, therefore, it may be necessary to consider the A_2 term. An upper limit for the possible error in the molar mass determination was estimated as follows. The largest amylopectin molecules detected (which would have the largest error in their estimated molar mass because of to their A_2 term being neglected) have molar masses of approximately 10^9 g mol^{-1}. The concentration of this material in the cell is no higher than 10^{-6} g mL^{-1}. The second virial term is very seldom larger than 10^{-4} g mol mL for polysaccharides in water. In these circumstances, calculation of the molar mass by use of Eq. (4) gives an error of approximately 20%, which is a worst case scenario. Hence the error is likely to be substantially lower. If, however, it is of interest to eliminate the error, the A_2 term can be estimated by MALS batch measurements on amylopectin and amylose.

The Rayleigh–Gans–Debye (RGD) approximation, which is applied in the Astra software, is not strictly valid for objects of sizes comparable with the wavelength (633 nm) of the light, for example for amylopectin, and the Mie theory of light scattering may have to be applied.

Table 3 Crossflow rates that form an approximately exponentially decreasing cross flow with a half life of 4 min. These step-wise decreasing flow data were programmed into the Eclipse software

Time (min)	Crossflow rate (mL min^{-1})
0	1.00
1	0.84
2	0.71
3	0.59
4	0.50
5	0.42
6	0.35
7	0.30
8	0.25
9	0.21
10	0.18
11	0.15
12	0.13
14	0.11
17	0.07
18	0.04
19	0.00

The calculations of molar mass in this work assumed, however, that the RGD approximation was valid. The latest eluted components in the starch samples are very large and for them, therefore, the calculations may not be very accurate.

Results and discussion

A representative result is illustrated in Fig. 1. It shows the RI-signal fractogram and the MALS 90°-signal fractogram of a maize starch having normal amylose content (maize-1). Also shown are the molar masses and rms radii obtained, and, in addition, an axis that allows reading of the hydrodynamic diameters. The latter could not be obtained directly from Eq. (3), because a programmed crossflow was used. Instead the hydrodynamic diameter scale was calculated by a procedure described above ("Theory" section). In Fig. 2 there is a plot of the crossflow gradient; this applies to all other figures also, because the experimental conditions were identical. In the RI fractogram, for which the detector signal is proportional to the starch mass concentration, two maxima from two incompletely resolved size populations were observed. The first population (Population 1) peaks at 1.8 min and has lower hydrodynamic diameters than the second, peaking at 9.5 min (cf. Eq. (2)). In the MALS 90° fractogram, for which the detector signal is proportional both to the starch mass concentration and to the starch molar mass (cf. Eq. (4)), only the second population (Population 2) was revealed. The first population was invisible because it contains such low molar mass components that their light-scattering intensity became very low and could not be distinguished from the MALS detector noise. For this reason the molar mass data had acceptable precision only down to approximately ~ 3×10^6 g mol^{-1}. Determination of the molar mass and the rms radius was therefore possible only for the second population, which is further caused by the fact that for the first size population the angular dependence of the scattering intensity is too weak (the size of the eluted material is close to or below the size limit for determination of the rms radius).

In the RI fractograms of all the starch samples (Figs. 1, 2, 3, 4, 5, 6), the first population peak maximum was eluted after approximately 2 min whereas the second population peak maximum was eluted in the range 4–10 min. This shows, directly, characteristic differences between molecular hydrodynamic size. Most of the first population had molar masses $<10^6$ g mol^{-1}, whereas most of the second population had molar masses $>10^7$ g mol^{-1}. According to the literature, amylose often has a weight-average molar mass in the range 10^5–10^6 g mol^{-1} and amylopectin in the range 10^7–10^9 g mol^{-1} [9, 10]. This confirms that the first population was mainly amylose and the second mainly amylopectin. This was further supported by the fact that (see below) in the RI fractograms of the high-amylose starches (Figs. 2 and 5), the relative amount of the first population was much higher than in starch with normal amylose content whereas in the high-amylopectin starches the relative amount of the second population was much higher (Figs. 2 and 4).

The borderline between the two size populations was defined as the elution time at the minimum between them. If there was no well-defined minimum the borderline was taken as the point where the steep fronting up-slope of the second population started, or else where the steep trailing down-slope of the first population appeared to have ended.

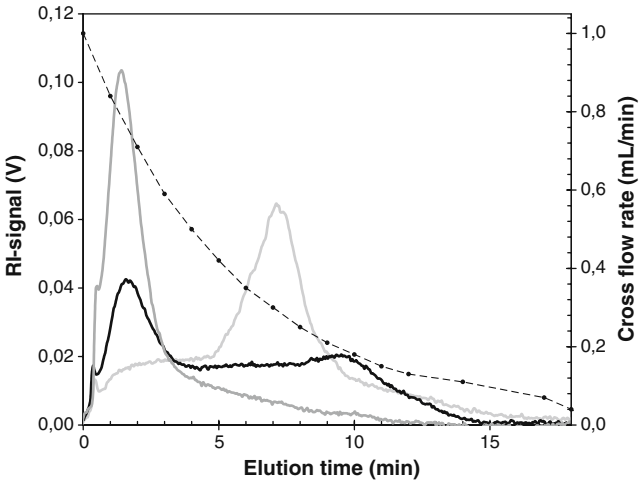

Fig. 2 RI-signal fractograms of three different maize starches: *dark grey line*, high-amylose (maize-2); *black line*, normal (maize-1); and *light grey line*, high-amylopectin (maize-3). The *dashed line* shows the crossflow gradient (this applies to all the other figures)

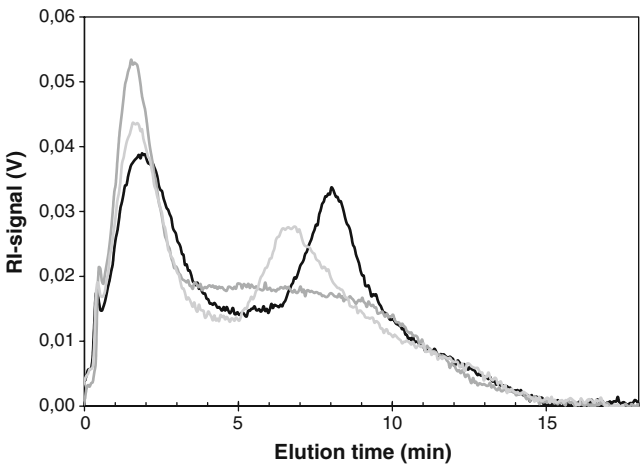

Fig. 3 RI-signal fractograms of three de-glutinised wheat starches: *black line*, wheat-4; *dark grey line*, wheat-5; and *light grey line*, wheat-6

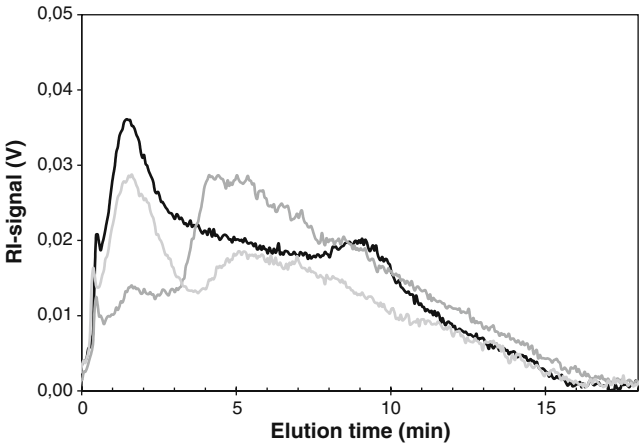

Fig. 4 RI-signal fractograms of three different rice starches: *black line*, normal rice (rice-10); *dark grey line*, high-amylopectin rice (rice-11); and *light grey line*, normal rice (rice-12)

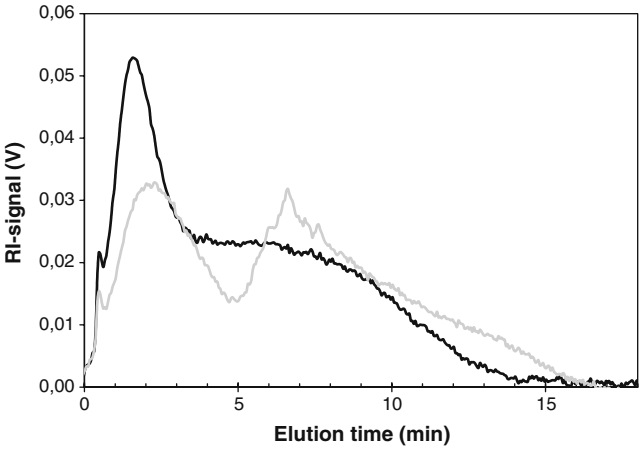

Fig. 6 RI-signal fractograms of, *black line*, tapioca (tapioca-8) and, *light grey line*, pea (pea-9) starches

The two starch polysaccharides are known to have different molecular shape (linear vs. branched) which should affect the relationship between the molar mass and the elution time, i.e. between the molar mass and the hydrodynamic diameter (cf. Eqs. (1) and (3)). This may cause amylose and amylopectin to have similar hydrodynamic diameter and, therefore, similar elution times, even if they have widely different molar mass [25]. This means that the two observed size populations cannot be referred to as pure amylose and pure amylopectin, respectively, which is similar to when size-exclusion chromatography is used [25].

The z-average rms radii for the second populations ranged from 140 to 320 nm (Table 2) and are of the same order as found previously for maize and barley starch [26, 27]. The hydrodynamic diameter intervals for the second size populations occurred in the range 24–550 nm, depending on the plant source, as judged from the hydrodynamic diameter axis in Fig. 1 when applied to all the other figures. The weight-average molar mass of the second population ranged from 45 to 450×10^6 g mol^{-1} depending on the plant source (Table 2).

There was no good correlation between the amylose contents given in Table 1 and the relative amounts of the amylose-rich population and the amylopectin-rich population calculated from the areas under the peaks. This discrepancy may in part be because of difficulties in defining the RI signal baseline and that it did not reach zero between populations. Further, the two populations may not be pure regarding amylose and amylopectin.

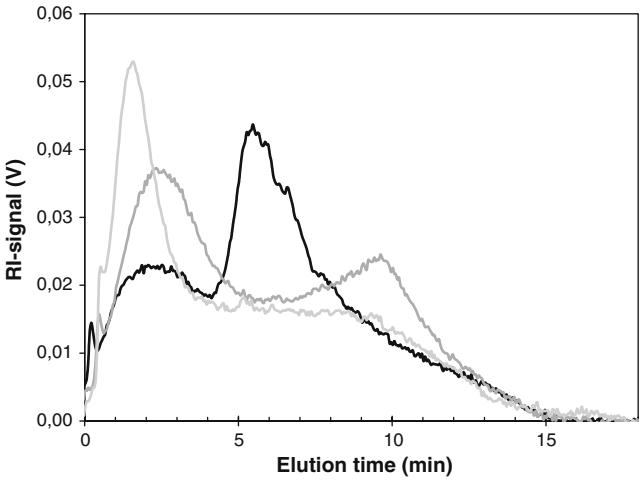

Fig. 5 RI-signal fractograms of three different potato starch samples: *black line*, normal potato (potato-7); *dark grey line*, low phosphate (potato-39); and *light grey line*, high-amylose (potato-40)

Maize starches

Comparison of the RI fractograms obtained from the three different maize starches (high-amylose, and normal and high-amylopectin) in Fig. 2 clearly shows that there was a much larger absolute and relative amount of the first size population (mainly amylose) in the high-amylose maize than in the normal maize and the high-amylopectin maize. The latter had a very low content of the first size population. Conversely there was a very low absolute and relative amount of the second population (mainly amylopectin) in the high-amylose maize compared with the other two. The normal maize showed intermediate character regarding the relative amounts of Population 1 and Population 2. This reflects very well the expected differences between the three maize types. Moreover, the weight-average molar mass of Population 2 (Table 2) was in the known range for amylopectin. It is interesting to note that the RI fractograms in Fig. 2 reveal the presence of small amounts of amylopectin in the high-

amylose maize and small amounts of amylose in the high-amylopectin maize.

Wheat starches

The RI fractograms obtained from three different deglutinised wheat starches (wheat-4, 5, and 6) were rather similar to each other in terms of the absolute amounts of the first population (the area under the curves in Fig. 3), which reflects the identical amylose contents (Table 1). They all had two clear size populations, although with somewhat different hydrodynamic size characters for the second population. The second population of wheat-5 had a lower weight-average molar mass than the other two and did not form a maximum in the elution curve.

Rice starches

Comparison of the RI fractograms (Fig. 4) obtained from the three different rice starches shows that the high-amylopectin rice starch (rice-11) had a relatively much lower amount of the first population and a much higher amount of the second population than the two normal starches (rice-10 and rice-12). This confirms expectations for a high-amylopectin variety.

For the second population the weight-average molar masses were similar, in the range $3.5–4.5\times10^8$ g mol^{-1} for all three samples. Rice-11 and rice-12 had similar rms radii of ~230 nm, whereas rice-10 had a higher value, 320 nm. Perhaps this is related to the fact that the peak of the second population of rice-10 occurred much later than for rice-11 and rice-12. In other words, rice-10 has a very different hydrodynamic diameter distribution of the second population.

Potato starches

All three potato starches had two clear size populations as judged from the two peak maxima (Fig. 5). The weight-average molar mass of the second population was not very different among the three starches (Table 2), yet their RI signals peaked at quite different elution times. The relative amount, as judged from the area under the curves in Fig. 5, of the first population in the high-amylose potato (potato-40) was rather similar to that in the low-phosphate starch of the same cultivar Dianella but somewhat higher than in the normal potato cultivar Kuras.

Tapioca starch

The tapioca starch had two size populations in the RI fractogram (tapioca-8 in Fig. 6). The second population did not form a maximum and had a weight-average molar mass of 6.1×10^7 g mol^{-1}.

Pea starch

Pea starch had two well-defined size populations in the RI fractogram (pea-9 in Fig. 6). The weight-average molar mass was 1.8×10^8 g mol^{-1} for the second size population.

Comparison among all starches

Large differences in starch characteristics were detected among varieties of the same species and among different botanical sources. Two size populations likely to contain mainly amylose (amylose-rich population) and mainly amylopectin (amylopectin-rich population), respectively, were found but they partially overlapped in most cases. This can be caused by co-elution of amylose and amylopectin in a range where they have similar hydrodynamic diameters. Another possibility is that this part represents intermediate material with characteristics between amylose and amylopectin [28–30]. The presence of an intermediate material has been described for high-amylose maize starch [11].

The relative amounts of the two populations correlated very well in most cases with the expected differences among high-amylose starch, normal starch, and high-amylopectin starch. Thus it is clear that on a qualitative level it is quite feasible to evaluate starch sample characteristics in terms of their amylose-to-amylopectin ratio. The amylose-rich populations had rather similar elution times for all starches, which is indicative of similar starch polymer size for these populations. For the amylopectin-rich populations there were clear maxima in the elution curves of high-amylose starch, normal starches, and high-amylopectin starches, with the exception of high-amylose maize (Maize-2), one of the deglutinised wheat starches (Wheat-5), high-amylose potato (Potato-40), and tapioca starch. For the latter, the elution curves were sloping all through the amylopectin-rich population.

The position of the peak maxima of the amylopectin-rich population varied a lot between the different starches but the tailing part seemed to end at about the same elution time for many of them. This shows that the largest starch polymer in each given starch was of about the same hydrodynamic size. Moreover, the tailing part was in many cases very long.

Comparison among tuber starches

Potato (potato-7) and tapioca starch (tapioca-8) had different characteristics with regard to population 2. This had a pronounced maximum at 4 min elution time in potato-7 but a sloping shoulder starting from 4 min in the tapioca starch (Figs. 5 and 6).

Conclusions

This study reveals the hydrodynamic size separation power of AsFlFFF–MALS–RI to generate a large number of molecular size characteristics data for different types of starch in a short time, thus making it suitable for screening of starch characteristics. In addition to the molar mass and rms radius it is clear that the hydrodynamic diameter is an important property which can be determined at different positions in the fractograms for example at the population peak maxima in Figs. 1, 2, 3, 4, 5, 6.

The data in this study can be used as starting point for more in-depth studies of the characteristics of starch than are presented here. Moreover, after mathematical transformation of the RI-signal fractograms in relation to the hydrodynamic diameter scale the weight distribution of hydrodynamic diameters can be obtained in the same way as the distribution of the diffusion coefficients [5]. If these were to be combined with the molar mass distributions interesting characteristics of the starch polymer conformations could be obtained. Further, the novel property "apparent density" (calculated from molar mass and the hydrodynamic diameter data) as introduced by Nilsson et al. [18] might further elucidate the character of the starch polymers especially in the range where amylose and amylopectin may be co-eluted.

It can be expected that future AsFlFFF-MALS-RI studies utilizing RI and MALS detectors with much reduced noise will enable the range of molar mass determinations to be stretched further into the amylose population.

Acknowledgements This work was financed by the project Øresund Starch Profile (ØSP) within Øforsk, headed by Denmark's Ministry for Science, Division of Technology and Development, and it was presented at the following meetings: the 29th International Symposium on High-Performance Liquid-Phase Separations and Related Techniques, June 26–30, 2005, Stockholm (Sweden), the 5th Annual Surface and Colloid Symposium on Amphiphilic Polymers 16–18 October 2005, Lund (Sweden), and the Fourth International Symposium on Separation and Characterization of Natural and Synthetic Macromolecules, 28–30 January 2009, Amsterdam (Netherlands).

References

1. Whistler R, BeMiller J, Paschall E (1984) Starch: chemistry and technology. Academic Press Inc., New York
2. Wahlund KG, Giddings JC (1987) Properties of an asymmetrical flow field-flow fractionation channel having one permeable wall. Anal Chem 59(9):1332–1339
3. Litzén A, Wahlund KG (1991) Zone broadening and dilution in rectangular and trapezoidal asymmetrical flow field-flow fractionation channels. Anal Chem 63(10):1001–1007
4. Litzen A (1993) Separation speed, retention, and dispersion in asymmetrical flow field-flow fractionation as functions of channel dimensions and flow-rates. Anal Chem 65(4):461–470
5. Wahlund KG, Litzen A (1989) Application of an asymmetrical flow field-flow fractionation channel to the separation and characterization of proteins, plasmids, plasmid fragments, polysaccharides and unicellular algae. J Chromatogr 461:73–87
6. Litzen A, Wahlund KG (1989) Improved separation speed and efficiency for proteins, nucleic-acids and viruses in asymmetrical flow field flow fractionation. J Chromatogr 476:413–421
7. Wahlund K-G (2000) Asymmetrical flow field-flow fractionation. In: Schimpf M, Caldwell K, Giddings JC (eds) Field-flow fractionation handbook. Wiley-Interscience, New York, pp 279–294
8. Lou JZ, Myers MN, Giddings JC (1994) Separation of polysaccharides by thermal field-flow fractionation. J Liq Chromatogr 17(14–15):3239–3260
9. Hanselmann R, Burchard W, Ehrat M, Widmer HM (1996) Structural properties of fractionated starch polymers and their dependence on the dissolution process. Macromolecules, vol 29
10. Hanselmann R, Ehrat M, Widmer HM (1995) Sedimentation field-flow fractionation combined with multi- angle laser-light scattering applied for characterization of starch polymers. Starch–Starke 47(9):345–349
11. Roger P, Baud B, Colonna P (2001) Characterization of starch polysaccharides by flow field - flow fractionation -multi-angle laser light scattering-differential refractometer index. J Chromatogr A 917(1–2):179–185
12. Kim WJ, Eum CH, Lim ST, Han JA, You SG, Lee S (2008) Separation of amylose and amylopectin in corn starch using dual-programmed flow field-flow Fractionation (vol 28, pg 2489, 2007). Bull Korean Chem Soc 29(4):894–894
13. You S, Stevenson SG, Izydorczyk MS, Preston KR (2002) Separation and characterization of barley starch polymers by a flow field - flow fractionation technique in combination with multiangle light scattering and differential refractive index detection. Cereal Chem 79(5):624–630
14. van Bruijnsvoort M, Wahlund KG, Nilsson G, Kok WT (2001) Retention behavior of amylopectins in asymmetrical flow field - flow fractionation studied by multi-angle light scattering detection. J Chromatogr A 925(1–2):171–182
15. Rolland-Sabate A, Colonna P, Mendez-Montealvo MG, Planchot V (2007) Branching features of amylopectins and glycogen determined by asymmetrical flow field flow fractionation coupled with multiangle laser light scattering. Biomacromolecules 8 (8):2520–2532. doi:10.1021/bm070024z
16. Wittgren B, Wahlund KG, Derand H, Wesslen B (1996) Aggregation behavior of an amphiphilic graft copolymer in aqueous medium studied by asymmetrical flow field-flow fractionation. Macromolecules 29(1):268–276
17. Leeman M, Wahlund KG, Wittgren B (2006) Programmed cross flow asymmetrical flow field-flow fractionation for the size separation of pullulans and hydroxypropyl cellulose. J Chromatogr A 1134(1–2):236–245. doi:10.1016/j.chroma.2006.08.065
18. Nilsson L, Leeman M, Wahlund KG, Bergenstahl B (2006) Mechanical degradation and changes in conformation of hydrophobically modified starch. Biomacromolecules 7(9):2671–2679. doi:10.1021/bm060367h
19. Rayleigh L (1910) The incidence of light upon a transparent sphere of dimensions comparable with the wave-length. Proc R Soc Lond Ser Containing Pap Math Phys Character 84(567):25–46
20. Einstein A (1910) Opalescence theory of homogeneous liquids and liquid mixtures in the vicinity of the critical state. Annalen der Physik (Weinheim, Germany) 33:1275–1298
21. Wyatt PJ (1993) Light scattering and the absolute characterization of macromolecules. Anal Chim Acta 272(1):1–40
22. Andersson M, Wittgren B, Wahlund KG (2003) Accuracy in multiangle light scattering measurements for molar mass and radius estimations. Model calculations and experiments. Anal Chem 75(16):4279–4291. doi:10.1021/ac030128+

23. Jackson DS (1991) Solubility behavior of granular corn starches in methyl sulfoxide (DMSO) as measured by high-performance size exclusion chromatography. Starch–Starke 43(11):422–427
24. Bradbury AGW, Bello ABT (1993) Determination of molecular-size distribution of starch and debranched starch by a single procedure using high-performance size-exclusion chromatography. Cereal Chem 70(5):543–547
25. Buleon A, Colonna P, Planchot V, Ball S (1998) Starch granules: structure and biosynthesis. Int J Biol Macromol 23(2):85–112
26. Han JA, Lim H, Lim ST (2005) Comparison between size exclusion chromatography and micro-batch analyses of corn starches in DMSO using light scattering detector. Starch–Starke 57(6):262–267
27. You SG, Izydorczyk MS (2002) Molecular characteristics of barley starches with variable amylose content. Carbohydr Polym 49(1):33–42
28. Baba T, Arai Y (1984) Structural features of amylomaize starch.3. structural characterization of amylopectin and intermediate material in amylomaize starch granules. Agric Biol Chem 48(7):1763–1775
29. Banks W, Greenwoo Ct, Muir DD (1974) Studies on starches of high amylose content .17. A review of current concepts. Starke 26 (9):289–300
30. Bertoft E, Qin Z, Manelius R (1993) Studies on the structure of pea starches .4. intermediate material of wrinkled pea starch. Starch–Starke 45(12):420–425